

# Catalysis Science & Technology

Accepted Manuscript



This is an *Accepted Manuscript*, which has been through the Royal Society of Chemistry peer review process and has been accepted for publication.

*Accepted Manuscripts* are published online shortly after acceptance, before technical editing, formatting and proof reading. Using this free service, authors can make their results available to the community, in citable form, before we publish the edited article. We will replace this *Accepted Manuscript* with the edited and formatted *Advance Article* as soon as it is available.

You can find more information about *Accepted Manuscripts* in the [Information for Authors](#).

Please note that technical editing may introduce minor changes to the text and/or graphics, which may alter content. The journal's standard [Terms & Conditions](#) and the [Ethical guidelines](#) still apply. In no event shall the Royal Society of Chemistry be held responsible for any errors or omissions in this *Accepted Manuscript* or any consequences arising from the use of any information it contains.



Journal Name

ARTICLE

## Polydopamine Nanofilm as Visible Light-Harvesting Interfaces for Palladium Nanocrystals Catalyzed Coupling Reactions

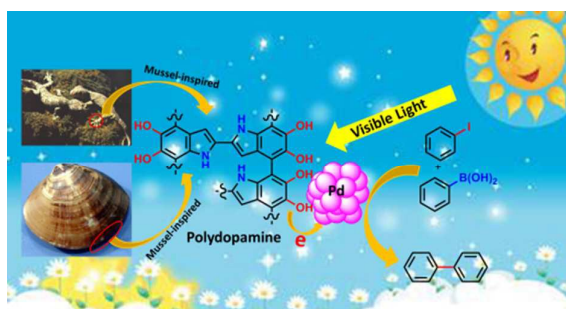
Aming Xie,<sup>\*ab</sup> Kun Zhang,<sup>c</sup> Fan Wu,<sup>\*b</sup> Nana Wang,<sup>b</sup> Yuan Wang,<sup>b</sup> and Mingyang Wang<sup>\*ab</sup>

Received 00th January 20xx,  
Accepted 00th January 20xx

DOI: 10.1039/x0xx00000x

www.rsc.org/

Light-harvesting material is of great importance for the efficient use of solar energy to driven catalytic reactions in chemistry. We herein report mussel-inspired polydopamine nanofilm as light-harvesting interfaces for heterogeneous palladium catalyzed coupling reactions under irradiation of visible light. Our strategy includes in situ growth of palladium nanocrystals on polydopamine nanofilm to prepare photocatalysts and photocatalytic Suzuki coupling reactions involving a broad range of aryl bromides/iodides and arylboronic acids substrates. The polydopamine based photocatalysts could be supported on various carriers regardless of the size or morphology, thus easily recycled and reused. A plausible photocatalytic mechanism has been proposed including light-harvesting, photoelectron-holes separation and transfer processes. This strategy also has potential in other noble metals such as platinum, indium and gold photocatalytic organic reactions such as couplings, reductions and oxidations.



### Introduction

Efficient harvesting of solar energy, a clean, abundant, and sustainable energy source, is of great importance in the future exploitation of new energies.<sup>1</sup> Up to now, there have mainly been three technologies for the capture and conversion of solar energy: photovoltaics, solar heating, and solar thermal electricity.<sup>2-4</sup> Apart from these technologies, the use of sunlight to drive chemical reactions, often called photocatalysis, is another important mean to harvest solar energy and shows great potential in various chemical

processes, such as photocatalytic degradation of pollutants where semiconductors are typically utilized to generate electrons/holes under light,<sup>5,6</sup> organic reactions photocatalyzed by Mott-Schottky heterojunctions,<sup>7</sup> Au-Pd alloy,<sup>3,8,9</sup> and Pd nanostructures.<sup>10,11</sup> Normally, photocatalysis processes refer efficient photogeneration and separation of electron-hole pairs which are the key factors for photosynthesis as well as light-driven chemical reactions.<sup>12-14</sup> Polydopamine (PDA) (Figure 1), a black mimic biopolymer inspired from mussel of shellfishes and geckos, have been displayed a very broad range of applications in the fields of energy, environment, and biomedicine, since its first use as a coating material in 2007.<sup>15-20</sup> As a synthetic eumelanin polymer, PDA possess a capability of light absorption under a broadband spectrum from UV to visible region.<sup>21-24</sup> The photoconductivity can be strongly enhanced under the radiation of visible light, implying the increase of photogenerated free electrons and electron holes.<sup>25</sup> As catechol derivatives, PDA can effectively transfer photoinduced electrons and protons which is crucial for the artificial photocatalysis systems, thus significantly improved the photocatalytic activity, such as

<sup>a</sup> School of Mechanical Engineering, Nanjing University of Science & Technology, Nanjing 210094, China. E-mail: aminghugang@126.com, wmyrf@163.com.

<sup>b</sup> State Key Laboratory for Disaster Prevention & Mitigation of Explosion & Impact, PLA University of Science and Technology, Nanjing 210007, China. E-mail: wufanjlg@163.com

<sup>c</sup> School of Chemical Engineering, Nanjing University of Science & Technology, Nanjing 210094, China.

Electronic Supplementary Information (ESI) available: [Preparation process of carbonized loofah (CL), catalysts recovery experiments, XRD results, NMR data and NMR spectra]. See DOI: 10.1039/x0xx00000x

photochemical oxidation of water, and photodegradation of organic dyes, though independent photoactive reagents were required.<sup>26,27</sup> The photoexcited electron in PDA can be injected into wide bandgap semiconductor such as TiO<sub>2</sub> nanoparticles, thus resulted enhanced photovoltaic conversion under solar light.<sup>28</sup> All these results above sufficiently demonstrate that PDA can provide efficient photogeneration, separation as well as transfer of electron-hole pairs under irradiation of visible light, implying a possibility of electron transfer to the conduction band of noble metals such as Pd, Pt, Rh, and Ir because of the zero energy gap. This light energy transformation of PDA may significantly improve the catalytic activity of noble metals and make PDA become a potential light harvesting material for photocatalysis. However, up to date, the use of PDA to effectively harvest and transform light energy for photocatalyzed reactions have been largely overlooked.

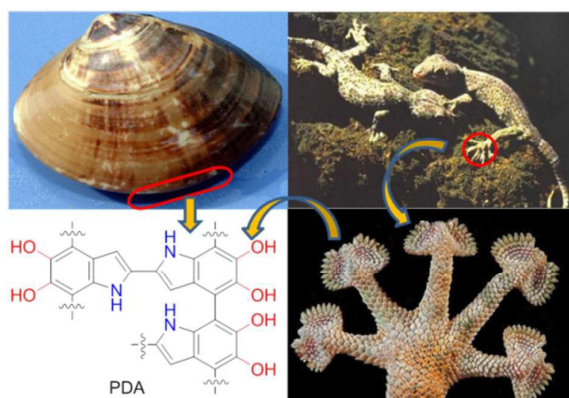


Figure 1. The structure of mussel-inspired PDA

Recently, by virtue of the facile recyclability and high efficiency, heterogeneous Pd nanocrystals (PNs) catalysts have been extensively developed for coupling reactions, such as the loading of PNs on carbon materials including graphene,<sup>29</sup> polymers including Poly(*N*-isopropylacrylamide),<sup>30</sup> and metal oxides including alumina oxides.<sup>31</sup> However, elevated temperature and prolonged reaction time must be required for these catalytic systems because the rate of the rate-limiting steps was restricted by the high activation barrier of substrates, thus leading to undesired side products and instability of the catalysts. Ideal strategy to circumvent this insufficiency may be using energy of visible light to activate the reactants or catalysts at lower operating temperatures.<sup>32,33</sup> Herein, we describe a strategy to execute heterogeneous photocatalytic coupling reactions using PDA nano film as a light harvesting and transformation interface and PNs as a noble metal catalyst. In our strategy, photogenerated electron-hole pairs in PDA under irradiation of visible light separate along the PDA networks and then the electron transfers to the conduction band of PNs resulting improved catalytic activity. To execute this strategy, we firstly decorate PDA nanofilm on various carriers including carbonaceous materials, inorganic oxides or organic polymers, then support PNs on the surface of PDA nano film by an in-situ growth pathway, and finally take Suzuki coupling reactions as example

to demonstrate the efficiency and mechanism of this photocatalysis system.

## Results and discussion

Through the formation of a thin nanofilm on materials, PDA could be served as a versatile agent for the surface functionalization of various materials including metals, carbonaceous materials, oxides, and polymers, regardless of the size or morphology.<sup>34,35</sup> As a result, noble metal PNs could easily in situ nucleate and grow on the PDA-modified surfaces.<sup>36</sup> To simplify the recycling of catalysts, we firstly decorated PDA nanofilm onto the surface of CL, then supported PNs on the resulted PDA surface through an in situ nucleation and growth process which was similar to the previous work,<sup>3</sup> and finally prepared a Pd@PDA-CL catalyst. Pd@PDA-SG was prepared according to a similar process. The N and OH groups in PDA can offer chelating binding sites for noble metals, resulting enhanced affinity toward metal surface. Hence, the loading amounts of Pd NPs increased obviously, indicating an elevated utilization ratio of Pd source under the same condition (See Table S1 in Electronic Supplementary Information ESI). The Fourier transform infrared (FT-IR) spectra showed the appearance of O-H or N-H (around 3300 cm<sup>-1</sup>) and N-H (1270 cm<sup>-1</sup>) groups of PDA skeleton and the apparent disappearance of peak (1410 cm<sup>-1</sup>) belong to C-H bond of CL, implying successful modification of PDA thinfilm on CL (Figure 2a). In Figure 2b, the band around 3300 cm<sup>-1</sup> was designated to O-H or N-H group and significantly strengthened for PDA-SG, as well as the appearance of peak at 1512 cm<sup>-1</sup> which was attribute to the indole ring vibration of PDA skeleton, indicating the existence of PDA on SG.<sup>37</sup> Figure 2c and d showed the SEM images of Pd@PDA-CL and Pd@PDA-SG, respectively. It was found that Pd particles distributed on the surfaces of CL and SG with sizes smaller than 100 nm.

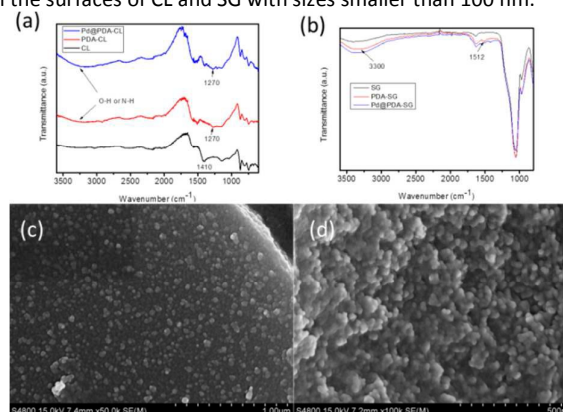
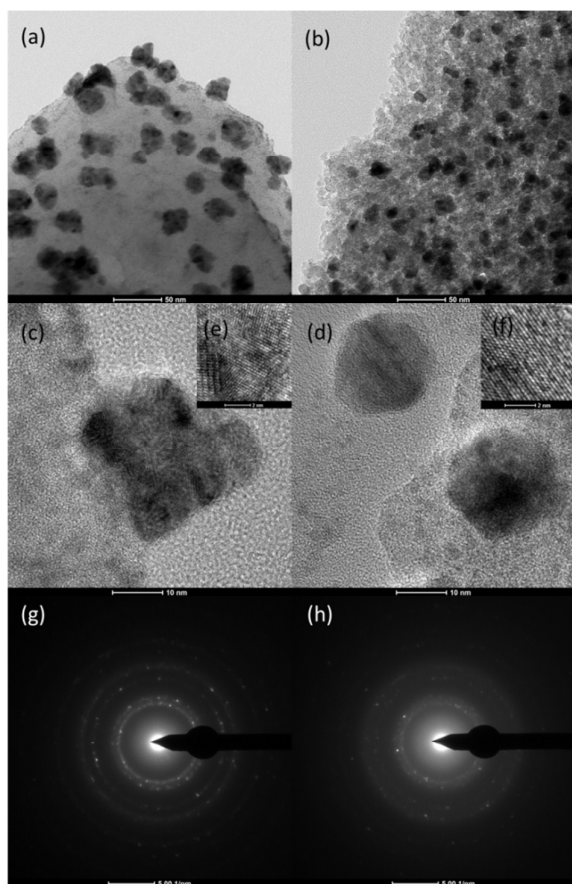


Figure 2. (a) FT-IR spectra of CL, PDA-CL and Pd@PDA-CL; (b) FT-IR spectra of SG, PDA-SG and Pd@PDA-SG; (c) SEM image of Pd@PDA-CL; (d) SEM image of Pd@PDA-SG.

To further explore the morphologies, sizes and crystals of Pd nano particles (NPs) supported on carriers, high-resolution transmission electron microscopy (HRTEM) imaging was used and the images were showed in Figure 3. The snail-shaped PNs distributed evenly on the PDA-modified surface of the lumpy CL with sizes ranged from 10 to 30 nm (Figure 3a and c), while PNs were spheres with an average size of 20 nm (Figure 3b and d). It can be inferred from the

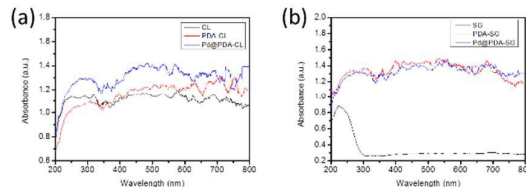
crystal lattice pattern that the PNs might be composed of randomly oriented small nanocrystals instead of single crystal when CL was employed as carrier (Figure 3e). On the contrary, SG was benefit for the formation of regular PNs (Figure 3b and d). These results can be attributed to different surface topography which influenced the growth process of PNs. The selected area electron diffraction (SAED) patterns also indicated that the PNs were polycrystals other than single crystals, regardless of carriers (Figure 3g and h). The X-ray scattering pattern (XRD) showed that supported PNs possessed consistent crystal faces (111), (200), and (220) with single-crystalline Pd nanoparticles (Figure S1 in ESI).<sup>38</sup>



**Figure 3.** (a,c,e) HRTEM images, (g) SAED pattern of Pd@PDA-CL; (b,d,f) HRTEM images, (h) SAED pattern of Pd@PDA-SG.

Next we used UV/vis diffuse reflection (UV/vis DR) spectra to study the visible light absorption of Pd@PDA photocatalysts. Normally, nonplasmonic Pd NPs showed a mild absorption toward visible light.<sup>11</sup> After supporting on PDA, the absorption intensity was increased slightly for Pd@PDA-CL (Figure 4a), because the black CL materials was of excellent light absorption ability. To avoid the interference of carrier, white particles SG with a negligible absorption in visible region was used and the absorption toward visible light enhanced enormously for Pd@PDA-SG (Figure 4a and b), indicating an excellent light-harvesting ability for PDA nanofilm. The electron paramagnetic resonance (EPR) showed an increased intensity of Pd@PDA-CL under visible light irradiation compared to

Pd@CL (Figure S2 in ESI), indicating a longer living photogenerated electron-hole pair inside Pd@PDA-CL than in Pd@CL.



**Figure 4.** (a) UV/vis DR spectra of CL, PDA-CL and Pd@PDA-CL; (b) UV/vis DR spectra of SG, PDA-SG and Pd@PDA-SG.

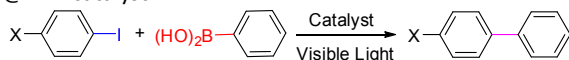
The coupling of iodobenzene with phenylboronic acid was chosen as a model reaction to explore the role of PDA and the photocatalytic activity of Pd@PDA catalyst. The coupling reaction proceeded well under white LED light irradiation whereas trace product was obtained in the dark (Table 1, entries 1,2). To avoid the photoheating effect, a control experiment under water bath was employed, but no apparent difference was observed (Table 1, entry 3). No reactions took place when PNs was taken off (Table 1, entry 4). These results above demonstrate a positive photocatalytic effect emerged during the coupling reaction. Nonplasmonic Pd NPs can exhibit apparent absorption of visible irradiation through the bound electrons and resulted excited conduction electrons, thus as a result displayed significant photocatalytic activity.<sup>11</sup> Nevertheless, supporting PNs on carbon material CL to form Pd@CL catalyst severely destroyed the photocatalytic activity without loss the thermocatalytic activity which was similar to commercial Pd/C catalyst (Table 1, entries 5-8), whereas Pd NPs supported on ZrO<sub>2</sub> powder did not decrease the photocatalytic activity.<sup>11</sup> This phenomenon may be originated from the strong absorption of light by black CL which prevents the light harvesting by PNs and the negligible light absorption at wavelengths longer than 370 nm. It can be also inferred that black CL cannot generate efficient photoexcited electrons under irradiation of visible light. The catalytic effect decreased with the reduction of catalyst amount (Table 1, entry 9). We also used another carrier SG to support PNs, and obviously, the employment of PDA significantly enhanced the light absorption and transformation for PNs catalyzed coupling reaction (Table 1, entries 10,11), which indicate enhanced photoexcitation and transfer of electron-hole pairs on the interface between PDA and PNs. Under the same condition, PS with three dimensional networks can also be used as the carrier for depositing PNs, implying a minor influence on carriers (Table 1, entry 12). In addition, some control experiments were adopted to understand the mechanism of the photocatalytic coupling, employing the use of radical and hole scavenger reagents (Table 1, entries 13-15). To distinguish the homocoupled products, 1-(4-iodophenyl)ethanone was taken as the model substrate instead of iodobenzene. The coupling reaction was greatly blocked with the addition of a radical scavenger 2,2,6,6-tetramethyl-1-piperidinyloxy (TEMPO) and a spot of homocoupled product 1,1'-([1,1'-biphenyl]-4,4'-diyl) diethanone appeared, inferring aggregation of 1-(4-iodophenyl) ethanone at the interface of PDA which can preferentially accept active electron from PNs (Table 1, entry 14). This aggregation effect can be observed by stirring of reaction mixture for 5-10 min. Via addition

## ARTICLE

Journal Name

of hole scavenger reagent diisopropylethylamine (DIPEA), where the hole was blocked, no target product 1-([1,1'-biphenyl]-4-yl)ethanone was obtained as well as homocoupled side product (Table 1, entry 15). This phenomenon may be attributed to stronger affinities of DIPEA to holes which prevent the combination of aryl boronic acid with hole.

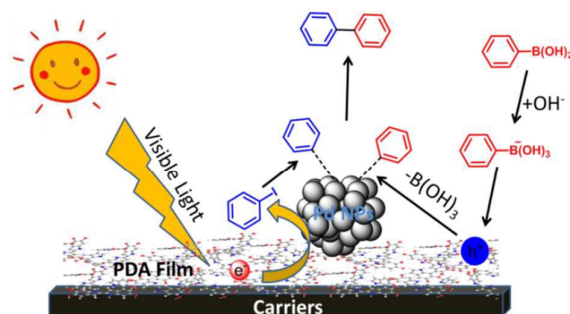
**Table 1.** Photocatalytic Suzuki Coupling Reaction Using Pd@PDA catalyst<sup>a</sup>



Entry	X	Catalyst	Light	Yield <sup>b</sup> (%)
1	H	Pd@PDA-CL	-	Trace <sup>c</sup>
2	H	Pd@PDA-CL	+	96
3	H	Pd@PDA-CL	+	94 <sup>d</sup>
4	H	PDA-CL	+	0
5	H	Pd@CL	+	Trace
6	H	Pd@C	+	17 <sup>e</sup>
7	H	Pd@PDA-CL	-	92 <sup>f</sup>
8	H	Pd@CL	-	90 <sup>f</sup>
9	H	Pd@PDA-CL	+	86 <sup>g</sup>
10	H	Pd@PDA-SG	+	92
11	H	Pd@PDA-SG	+	58
12	H	Pd@PDA-PS	+	90
13	Acetyl	Pd@PDA-CL	+	97
14	Acetyl	Pd@PDA-CL	+	68 <sup>h</sup>
15	Acetyl	Pd@PDA-CL	+	0 <sup>i</sup>

<sup>a</sup> Reaction conditions: iodobenzene (1 mmol), phenylboronic acid (1.1 mmol), K<sub>2</sub>CO<sub>3</sub> (1.5 mmol), catalyst (contained 0.6 mg of Pd), DMF/H<sub>2</sub>O (3 mL/3 mL), white LED lamp (1.2 W/cm<sup>2</sup>), room temperature, 2 h. <sup>b</sup> Isolated yields. <sup>c</sup> In dark, 6 h. <sup>d</sup> Water bath. <sup>e</sup> Commercial 5 wt % Pd@C catalyst (12 mg). <sup>f</sup> Carried at 100 °C. <sup>g</sup> catalyst (contained 0.3 mg of Pd). <sup>h</sup> Equivalent TEMPO was added, 54 % yield of 1-([1,1'-biphenyl]-4-yl)ethanone and 14% yield of 1,1'-([1,1'-biphenyl]-4,4'-diyl) diethanone. <sup>i</sup> Equivalent DIPEA was added.

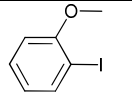
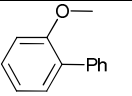
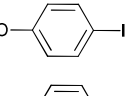
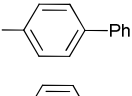
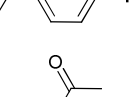
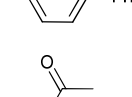
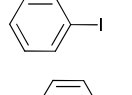
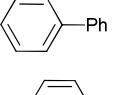
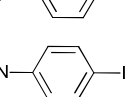
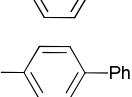
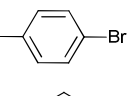
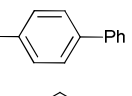
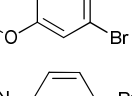
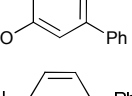
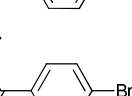
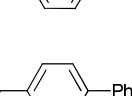
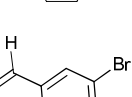
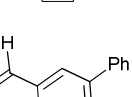
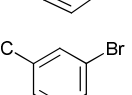
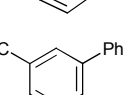
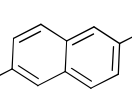
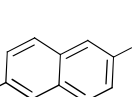
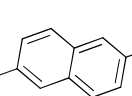
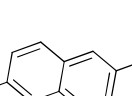



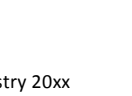
We proposed a plausible mechanism for the photocatalyzed Suzuki coupling reactions based on the observations from the experiments above and previous researches (Figure 5). As a semiconductor with a narrow band gap,<sup>28</sup> PDA film firstly absorbs visible light and generates electron-hole pairs. The photoexcited electrons in PDA diffuse to the PNs and lead to separation of excited charges (accumulation of negative charges on Pd metal whereas positive charges on PDA) due to the smaller work function of PDA than most noble metals including Pd.<sup>39</sup> Due to the excellent affinity of PDA toward organic and inorganic materials, iodobenzene molecules aggregate nearby the PDA interface and can be easily attacked by the PNs active center which lead to the formation of aryl complex with Pd. Meanwhile, the holes inside the PDA film activate the C-B bond of electronically negative B(OH)<sup>3-</sup> species which produced from the catching of OH<sup>-</sup> in the basic reaction medium by phenylboronic acid and another aryl Pd complex formed. Finally, the coupling product is formed via the reductive elimination and transmetalation processes which take place in typical Pd-catalyzed Suzuki reactions.<sup>3,40</sup>

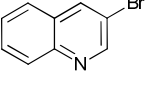
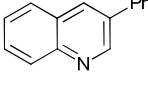
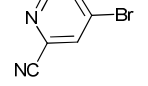
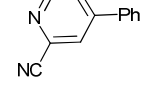


**Figure 5.** Proposed mechanism for the photocatalytic Suzuki coupling at the interface of PDA and Pd NPs.

To investigate the reaction scope, a series of aryl halides bearing a broad range of substituents have been employed to test the photocatalytic activity of Pd@PDA. As shown in Table 2, the substrates bearing electron-donating groups such as -OCH<sub>3</sub> and electron-withdrawing group such as -COCH<sub>3</sub> can react with phenylboronic acid smoothly to furnish corresponding coupling products in excellent yields (Table 2, entries 1-3). Prolonged time was required for the substrate 1-(2-iodophenyl) ethanone if want to obtain high yield of product (Table 2, entry 4). This phenomenon can be attributed to the increased steric effect of the -COCH<sub>3</sub> at the ortho-position. Due to -NH<sub>2</sub> can attack the catechol groups in PDA,<sup>35</sup> the substrate 4-iodoaniline was not be suitable for our photocatalytic system (Table 2, entry 5). Similar to DIPEA, -N(CH<sub>3</sub>)<sub>2</sub> can also capture the photoexcited holes preferentially, thus prevent the reaction of phenylboronic acid with 4-iodo-*N,N*-dimethylaniline (Table 2, entry 6). Apart from aryl iodides, various aryl bromides bearing substituents regardless of electron-donating groups or electron-withdrawing groups can be used as the substrates in our photocatalytic system (Table 2, entries 7-14). -F cannot be replaced by aromatic ring under the irradiation of visible light because only 4-fluoro-1,1'-biphenyl was isolated (Table 2, entry 7). The existence of naphthalene moieties did not influence the photocatalytic coupling reaction (Table 2, entries 13 and 14). The substrates bearing *N*-heterocycle moieties showed lower reaction activities toward phenylacetylene, partially owing to the self-substitution-reactions between N and Br atoms (Table 2, entries 15 and 16).

**Table 2.** The scope of aryl halides for photocatalytic Suzuki Coupling Reactions<sup>a</sup>

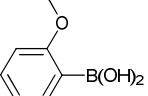
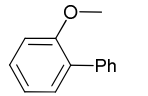
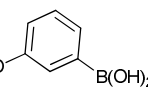
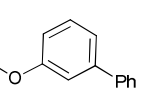
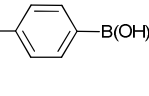
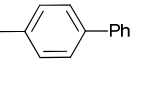
Aryl-X + (HO) <sub>2</sub> B-Ph		$\xrightarrow[\text{Visible Light}]{\text{Pd@PDA-CL}}$ Aryl-Ph	
Entry	Aryl Halide	Product	Yield <sup>b</sup> (%)
1			95
2			96
3			90
4			98 <sup>c</sup>
5			0 <sup>d</sup>
6			0 <sup>d</sup>
7			99
8			92
9			93
10			95
11			99
12			96
13			91
14			99

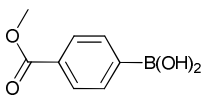
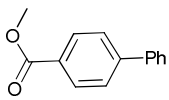
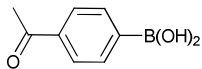
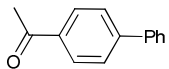
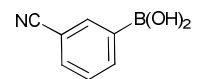
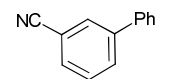
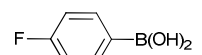
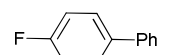
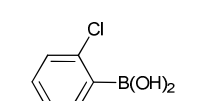
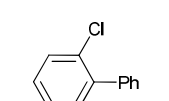
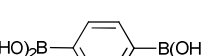
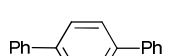
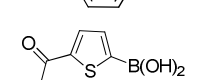
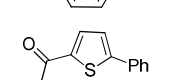
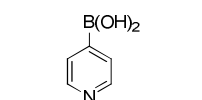
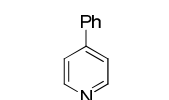
15			30
16			0

<sup>a</sup> Reaction conditions: aryl halide (1 mmol), phenylboronic acid (1.1 mmol), K<sub>2</sub>CO<sub>3</sub> (1.5 mmol), Pd@PDA-CL (20 mg, 3 wt % Pd content), DMF/H<sub>2</sub>O (3 mL/3 mL), white LED lamp (1.2 W/cm<sup>2</sup>), room temperature, 2 h. <sup>b</sup> Isolated yields. <sup>c</sup> 10 h. <sup>d</sup> No coupling product was monitored by TLC.

In addition, various aryl boronic acids have been used to explore the scope of our photocatalytic system. As shown in Table 3, aryl boronic acids bearing electron-rich groups and electron-deficient groups smoothly react with iodobenzene to form corresponding coupling products in excellent yields (Table 3, entries 1-6). -F and -Cl can be retained under the reaction condition, indicating that this technique was suitable for aryl fluorides/chlorides (Table 3, entries 7-8). Furthermore, 1,4-phenylenediboronic acid was appropriate substrate in our photocatalytic system, implying tremendous potential in noble metal catalyzed polymerization (Table 3, entry 9). The Pd@PDA-CL catalyzed coupling reaction cannot be prevented when the bromobenzene was employed instead of iodobenzene (Table 3, entries 1, 3, 5, 7 and 10). For *S*-heterocycle boronic acids, moderate yield of coupling product can be isolated (Table 3, entry 10). However, the reaction of bromobenzene with substrate bearing *N*-heterocycle moiety cannot take place because the reduced electron density prevented the combination of boric acid with photogenerated holes (Table 3, entry 11). After carrying the photocatalytic reaction, the Pd@PDA-CL catalyst can be easily recycled by filtration and washing with solvents without significantly Pd loss (Table S2 in ESI). The recycled can be reused without apparent reduction of photocatalytic activity no less than five times (Table S2 in ESI).

**Table 3.** The scope of aryl boronic acids for photocatalytic Suzuki Coupling Reactions<sup>a</sup>

Ph-I/Br + (HO) <sub>2</sub> B-Aryl		$\xrightarrow[\text{Visible Light}]{\text{Pd@PDA-CL}}$ Ph-Aryl	
Entry	Aryl Boronic Acid	Product	Yield <sup>b</sup> (%)
1			93 <sup>c</sup> , 90 <sup>d</sup>
2			88 <sup>c</sup>
3			99 <sup>c</sup> , 96 <sup>d</sup>

4			93 <sup>c</sup>
5			90 <sup>c</sup> , 94 <sup>d</sup>
6			98 <sup>c</sup>
7			91 <sup>c</sup> , 88 <sup>d</sup>
8			95 <sup>c</sup>
9			97 <sup>c</sup>
10			75 <sup>d</sup>
11			0 <sup>d</sup>

<sup>a</sup> Reaction conditions: aryl halide (1 mmol), phenylboronic acid (1.1 mmol), K<sub>2</sub>CO<sub>3</sub> (1.5 mmol), Pd@PDA-CL (20 mg, 3 wt % Pd content), DMF/H<sub>2</sub>O (3 mL/3 mL), white LED lamp (1.2 W/cm<sup>2</sup>), room temperature, 2 h. <sup>b</sup> Isolated yields. <sup>c</sup> Iodobenzene was used as the substrate. <sup>d</sup> Bromobenzene was used as the substrate.

## Experimental

### Chemicals and Materials

All reagents and solvents were purchased from GENERAL-REAGENT, Titan Scientific Co., Ltd., Shanghai, China. and used without purification. Carbonized loofah (CL) was prepared by process seeing the Supporting Information for the preparation of CL. Distilled water was obtained from Direct-Q3UV, Millipore. Visible light was obtained for photocatalysis using two white LED lamps (12W) purchased from Philips Co., Ltd.

### General procedure for the growth of PNs on PDA nanofilm

Take CL carrier as an example: CL powder was added to a solution of dopamine (2 mg/mL) in 10 mM Tris-HCl (pH = 8.5) with stirring for 24 hours at room temperature. After filtration and washing with deionized water and acetone, a PDA nanofilm decorated CL material (PDA-CL) was obtained. Then, PDA-CL (1 g) was dispersed in water (100 mL) and mixed with acetone solution (50 mL) of Pd(OAc)<sub>2</sub> (100 mg). After stirring at 90 °C for 3 h, the resulting Pd@PDA-CL photocatalyst was obtained by filtration, washing with hot water and acetone, drying in vacuum. Other photocatalysts such as Pd@PDA-SG using silica gel (SG) instead of CL was through a similar process. ICP analysis: 3.2 wt% Pd for Pd@PDA-CL and 4.7 wt% Pd for Pd@PDA-SG.

### General procedure for the photocatalytic Suzuki coupling reaction by Pd@PDA photocatalysts

Take Pd@PDA-CL as an example: a mixture of iodobenzene (1 mmol), phenylboronic acid (1.1 mmol), K<sub>2</sub>CO<sub>3</sub> (1.5 mmol) and 20 mg Pd@PDA-CL (3.2 wt% Pd content) in 3 mL of DMF/H<sub>2</sub>O (Vol : Vol = 1 : 1) solution were stirred under argon with two white LED lamps (12 W) for a certain period of time. After the reaction, the catalyst was recycled by filtration and the organic phase of the filtrate was extracted with EtOAc, washed three times with water and dried over Na<sub>2</sub>SO<sub>4</sub>. The pure product was then isolated by silica chromatography using petroleum ether/ EtOAc mixtures as the eluent.

### Characterizations of Catalysts

UV-vis diffuse reflectance spectra were recorded at room temperature on a Thermo Fisher Scientific EV220 spectrophotometer. NMR measurements were recorded on Bruker AVANCE 500 (III) systems using CDCl<sub>3</sub> as the solvent. FT-IR spectra were recorded on a Nicolet iS10 FTIR instrument (Thermo Fisher Scientific, USA). The detailed morphologies of the photocatalysts were observed with a field emission scanning electron microscope (FE-SEM, S4800, Hitachi) and a field emission high resolution transmission electron microscope (FE-HRTEM, Tecnai G2 F20, FEI). Inductively coupled plasma analysis (ICP) was performed on a spectrometer (Optima 7300V, PerkinElmer). The crystal structure data of the as-synthesized samples was obtained from a X-ray diffractometer (XRD, D8 Advance, Bruker AXS) from 10° to 80°, using Cu Kα (λ = 1.54 Å) radiation. The electron paramagnetic resonance (EPR) spectra were obtained on a spectrometer (A300-10/12, Bruker). Flash column chromatography was performed by employing 200-300 mesh silica gel. Thin-layer chromatography (TLC) was performed with silica gel HSGF254.

## Conclusions

In summary, mussel-inspired polydopamine nanofilm has been developed as light-harvesting interfaces for heterogeneous palladium catalyzed coupling reactions under irradiation of visible light. Photocatalysts have been prepared by an in situ growth of palladium nanocrystals on polydopamine nanofilm and used for photocatalytic Suzuki coupling reactions involving a broad range of aryl bromides/iodides and arylboronic acids substrates. The polydopamine based photocatalysts could be supported on various carriers regardless of the size or morphology, thus easily recycled and reused. A plausible photocatalytic mechanism has been proposed including light-harvesting, photoelectron-holes separation and transfer processes. This strategy also has potential in other noble metals such as platinum, indium and gold photocatalytic organic reactions such as couplings, reductions and oxidations.

## Acknowledgements

The authors acknowledge the National Natural Science Foundation of China (NSFC 51403236 and 51021001) and State

Key Laboratory of Disaster Prevention & Mitigation of Explosion & Impact (DPMEIKF201310) for financially supporting this research.

## Notes and references

- N. S. Lewis and D. G. Nocera, *Proc. Natl. Acad. Sci. U.S.A.*, 2006, **103**, 15729.
- A. Shah, P. Torres, R. Tschärner, N. Wyrsh and H. Keppner, *Science*, 1999, **285**, 692.
- Z. J. Wang, S. Ghasimi, K. Landfester and K. A. I. Zhang, *Chem. Mater.*, 2015, **27**, 1921.
- D. Mills, *Sol. Energy*, 2004, **76**, 19.
- C. Yu, G. Li, S. Kumar, K. Yang and R. Jin, *Adv. Mater.*, 2014, **26**, 892.
- J. Zhao, C. Chen and W. Ma, *Top. Catal.*, 2005, **35**, 269.
- X. H. Li and M. Antonietti, *Chem. Soc. Rev.*, 2013, **42**, 6593.
- Q. Xiao, S. Sarina, E. Jaatinen, J. Jia, D. P. Arnold, H. Liu and H. Zhu, *Green Chem.*, 2014, **16**, 4272.
- Q. Xiao, S. Sarina, A. Bo, J. Jia, H. Liu, D. P. Arnold, Y. Huang, H. Wu and H. Zhu, *ACS Catal.*, 2014, **4**, 1725.
- R. Long, Z. Rao, K. Mao, Y. Li, C. Zhang, Q. Liu, C. Wang, Z. Li, X. Wu and Y. Xiong, *Angew. Chem. Int. Ed.*, 2015, **54**, 2425.
- S. Sarina, H. Zhu, Q. Xiao, E. Jaatinen, J. Jia, Y. Huang, Z. Zheng and H. Wu, *Angew. Chem. Int. Ed.*, 2014, **53**, 2935.
- S. H. Lee, J. H. Kim and C. B. Park, *Chem. Eur. J.*, 2013, **19**, 4392.
- J. H. Kim, M. Lee, J. S. Lee and C. B. Park, *Angew. Chem. Int. Ed.*, 2012, **51**, 517.
- J. Ryu, S. H. Lee, D. H. Nam and C. B. Park, *Adv. Mater.*, 2011, **23**, 1883.
- Y. Liu, K. Ai and L. Lu, *Chem. Rev.*, 2014, **114**, 5057.
- M. H. Ryu, J. Kim, I. Lee, S. Kim, Y. K. Jeong, S. Hong, J. H. Ryu, T. S. Kim, J. K. Park, H. Lee and J. W. Choi, *Adv. Mater.*, 2013, **25**, 1571.
- G. Kwon, A. K. Kota, Y. Li, A. Sohani, J. M. Mabry and A. Tuteja, *Adv. Mater.*, 2012, **24**, 3666.
- K. Kang, S. Lee, R. Kim, I. S. Choi and Y. Nam, *Angew. Chem. Int. Ed.*, 2012, **51**, 13101.
- J. Stritzker, L. Kirscher, M. Scadeng, N. C. Deliolanis, S. Morscher, P. Symvoulidis, K. Schaefer, Q. Zhang, L. Buckel, M. Hess, U. Donat, W. G. Bradley, V. Ntziachristos and A. A. Szalay, *Proc. Natl. Acad. Sci. U.S.A.*, 2013, **110**, 3316.
- H. Lee, S. M. Dellatore, W. M. Miller and P. B. Messersmith, *Science*, 2007, **318**, 426.
- I. F. Vecchia, P. Cerruti, G. Gentile, M. E. Errico, V. Ambrogio, G. D'Errico, S. Longobardi, A. Napolitano, L. Paduano, C. Carfagna and M. Dischia, *Biomacromolecules*, 2014, **15**, 3811.
- A. Pezzella, A. Iadonisi, S. Valerio, L. Panzella, A. Napolitano, M. Adinolfi and M. Dischia, *J. Am. Chem. Soc.*, 2009, **131**, 15270.
- C. T. Chen, C. Chuang, J. Cao, V. Ball, D. Ruch and M. J. Buehler, *Nat. Commun.*, 2014, **5**, 3859.
- M. Dischia, A. Napolitano, V. Ball, C. Chen and M. J. Buehler, *Acc. Chem. Res.*, 2014, **47**, 3541.
- A. B. Mostert, B. J. Powell, F. L. Pratt, G. R. Hansonc, T. Sarnad, I. R. Gentle and P. Meredith, *Proc. Natl. Acad. Sci. U.S.A.*, 2012, **109**, 8943.
- J. H. Kim, M. Lee and C. B. Park, *Angew. Chem. Int. Ed.*, 2014, **53**, 6364.
- J. J. Feng, P. P. Zhang, A. J. Wang, Q. C. Liao, J. L. Xi and J. R. Chen, *New J. Chem.*, 2012, **36**, 148.
- H. J. Nam, B. Kim, M. J. Ko, M. Jin, J. M. Kim and D. Y. Jung, *Chem. Eur. J.*, 2012, **18**, 14000.
- S. L. Buchwald, *Acc. Chem. Res.*, 2008, **41**, 1439.
- L. X. Yin and J. Liebscher, *Chem. Rev.*, 2007, **107**, 133.
- G. M. Scheuermann, L. Rumi, P. Steurer, W. Bannwarth and R. Mulhaupt, *J. Am. Chem. Soc.*, 2009, **131**, 8262.
- G. W. Wei, W. Q. Zhang, F. Wen, Y. Wang and M. C. Zhang, *J. Phys. Chem. C*, 2008, **112**, 10827.
- A. Gniewek, J. J. Ziolkowski, A. M. Trzeciak, M. Zawadzki, H. Grabowska and J. Wrzyszc, *J. Catal.*, 2008, **254**, 121.
- A. Postma, Y. Yan, Y. Wang, A. N. Zelikin, E. Tjpto and F. Caruso, *Chem. Mater.*, 2009, **21**, 3042.
- L. Q. Xu, W. J. Yang, K. G. Neoh, E. T. Kang and G. D. Fu, *Macromolecules*, 2010, **43**, 8336.
- L. Guo, Q. Liu, G. Li, J. Shi, J. Liu, T. Wang and G. Jiang, *Nanoscale*, 2012, **4**, 5864.
- A. Xie, F. Wu, M. Sun, X. Dai, Z. Xu, Y. Qiu, Y. Wang and M. Wang, *Appl. Phys. Lett.*, 2015, **106**, 222902.
- F. Wang, C. Li, L. D. Sun, C. H. Xu, J. Wang, J. C. Yu and C. H. Yan, *Angew. Chem. Int. Ed.*, 2012, **51**, 4872.
- S. Bai, J. Jiang, Q. Zhang and Y. Xiong, *Chem. Soc. Rev.*, 2015, **44**, 2893.
- Z. Jiao, Z. Zhai, X. Guo and X. Guo, *J. Phys. Chem. C*, 2015, **119**, 3238.